



# Sodium metasilicate ( $\text{Na}_2\text{SiO}_3$ ): A thermo-kinetic analysis of its $\text{CO}_2$ chemical sorption

Marco T. Rodríguez, Heriberto Pfeiffer\*

*Instituto de Investigaciones en Materiales, Universidad Nacional Autónoma de México, Circuito exterior s/n, CU Del. Coyoacán, CP 04510, México, DF, Mexico*

## ARTICLE INFO

### Article history:

Received 10 January 2008

Received in revised form 21 April 2008

Accepted 29 April 2008

Available online 4 May 2008

### Keywords:

Ceramics

Chemical sorption

Kinetics

Silicates and surface properties

## ABSTRACT

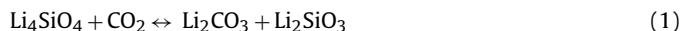
Sodium metasilicate ( $\text{Na}_2\text{SiO}_3$ ) was prepared by two different methods, solid-state reaction and precipitation. Then, samples were characterized by powder X-ray diffraction, scanning electron microscopy,  $\text{N}_2$  adsorption and thermogravimetric analysis. Thermal analyses showed that  $\text{Na}_2\text{SiO}_3$  has the capacity to absorb small quantities of  $\text{CO}_2$  between room temperature and  $130^\circ\text{C}$ . Modeling the surface reaction and sodium diffusion, the activation energies for these two processes were estimated to be  $17,482\text{ J/mol}$  and  $23,968\text{ J/mol}$ , respectively. Finally, the effect of the particle size, on the  $\text{CO}_2$  sorption, was found to be very important. The quantities of  $\text{CO}_2$  absorbed increased three times, when the particle size decreased and consequently the surface area increased.

© 2008 Elsevier B.V. All rights reserved.

## 1. Introduction

One of the principal world concerns, is related to pollution gases, and especially carbon dioxide ( $\text{CO}_2$ ) emissions [1,2]. In that way, in the last 10 years, several papers have shown that some alkaline ceramics, mainly lithium and sodium containing compounds, could be used as  $\text{CO}_2$  absorbents [3–10]. In general, these ceramics present a double-step sorption mechanism: a chemical sorption of  $\text{CO}_2$  over the ceramic surface, which produces an alkaline carbonate shell. Then, when the external shell is formed, the alkaline element diffuses throughout the carbonate external layer, to reach the surface and react with  $\text{CO}_2$  [8–10]. Therefore, one of the most important features of these materials is related to the diffusion of the alkaline element.

So far, among these compounds, lithium silicates, specifically lithium orthosilicate ( $\text{Li}_4\text{SiO}_4$ ) seems to be one of the best options to absorb  $\text{CO}_2$ . In this case, several authors have reported the  $\text{CO}_2$  capture through the following reaction [1,2,7,11–13].



Implicitly, these papers showed that  $\text{Li}_2\text{SiO}_3$  does not react. In fact, Kato and Nakagawa [14] tested this material for the  $\text{CO}_2$  capture. They did not observe any weight increment, and it was justified due to kinetic factors.

On the other hand, sodium ceramics have shown, in general, to be better  $\text{CO}_2$  absorbents in comparison to lithium ceramics. For example  $\text{Na}_2\text{ZrO}_3$  absorbs twice more  $\text{CO}_2$  than  $\text{Li}_2\text{ZrO}_3$ , and its reaction rate is faster as well [9]. Therefore, although  $\text{Li}_2\text{SiO}_3$  seems not to absorb  $\text{CO}_2$ ,  $\text{Na}_2\text{SiO}_3$  may have better reactivity. Then, the aim of this work was to study the thermal stability,  $\text{CO}_2$  sorption reactivity and particle size effect of  $\text{Na}_2\text{SiO}_3$ , through thermal analyses to obtain information about the  $\text{CO}_2$  sorption reactivity on  $\text{Na}_2\text{SiO}_3$ .

## 2. Experimental

Sodium metasilicate was synthesized by two different methods: solid-state reaction and precipitation. The solid-state reaction was performed with a mechanical mixture of silicon oxide ( $\text{SiO}_2$ , Aldrich) and sodium carbonate ( $\text{Na}_2\text{CO}_3$ , Aldrich) powders. Then, the mixture was calcined at  $900^\circ\text{C}$  for 4h. On the contrary, precipitation of  $\text{Na}_2\text{SiO}_3$  was produced from an aqueous solution of tetraethyl orthosilicate (TEOS,  $\text{Si}(\text{OC}_2\text{H}_5)_4$ , Aldrich) and sodium hydroxide ( $\text{NaOH}$ , Baker). Here,  $\text{NaOH}$  was dissolved in water as a first step. TEOS was, then, slowly added, drop by drop, to the solution. The mixture obtained was stirred and heated at  $70^\circ\text{C}$  until it dried. In this case,  $\text{Na}_2\text{SiO}_3$  was obtained without any further thermal treatment. This synthesis was performed to obtain small particles, and analyze the effect of the particle size on the  $\text{CO}_2$  absorption process. In both methods of synthesis the Na:Si molar ratio was equal to 2:1.

\* Corresponding author. Tel.: +52 55 5622 4627; fax: +52 55 5616 1371.  
E-mail address: [pfeiffer@iim.unam.mx](mailto:pfeiffer@iim.unam.mx) (H. Pfeiffer).

The samples were characterized by different techniques such as powder X-ray diffraction (XRD), scanning electron microscopy (SEM),  $N_2$  adsorption (BET) and thermogravimetric analysis (TGA). The XRD patterns were obtained with a BRUKER axS Advance D8 diffractometer coupled to a Cu anode X-ray tube. The  $K\alpha$  wavelength was selected with a diffracted beam monochromator, and compounds were identified conventionally using the JCPDS database. SEM (Stereoscan 440, Cambridge) was used to determine the particle size and morphology of the materials before and after the  $CO_2$  capture. The samples were covered with gold to avoid a lack of electrical conductivity. Surface area analyses were performed on Micromeritics Gemini 2360 equipment. Before the  $N_2$  adsorption process, the samples were out gassed in vacuum at  $100^\circ C$  for 12 h. Surface areas were calculated with the BET equation. Finally, different thermal analyses were performed in Hi-Res TGA 2950 thermogravimetric analyzer equipment from TA Instruments. A set of samples was heat-treated, with a heating rate of  $5^\circ C/min$ , from room temperature to  $1000^\circ C$ . These analyses were carried out into a  $CO_2$  flux (Praxair, grade 3.0), using 10 mg of sample in each analysis. Additionally, another set of samples was analyzed isothermally under the same  $CO_2$  atmosphere at  $80^\circ C$ ,  $100^\circ C$  and  $120^\circ C$  for 5 h.

### 3. Results and discussion

$Na_2SiO_3$  was prepared by solid-state and precipitation methods. Initially,  $Na_2SiO_3$  was prepared by solid-state reaction. The XRD pattern showed that the sample was pure  $Na_2SiO_3$  (Fig. 1A). On the contrary, the sample prepared by precipitation was not totally pure (Fig. 1B), another secondary phase was detected in small quantities,  $Na_6Si_2O_7$ . The formation of  $Na_6Si_2O_7$  is consistent with heterogeneities in the sample arising from areas locally richer in sodium, than the average. Nevertheless, this sample was not thermally treated to eliminate this secondary phase, in order to obtain smaller particles of  $Na_2SiO_3$  in comparison to the solid-state sample.

Both samples were studied by SEM. The particle size was measured using standard procedures. Micrographs of  $Na_2SiO_3$  obtained by the two methods showed morphological differences between them. The sample obtained by solid-state reaction showed large polyhedral particles with a particle size between  $50\ \mu m$  and  $100\ \mu m$  (Fig. 2A). Furthermore, the texture of these particles was highly dense. This kind of morphology corresponds very well with the solid-state reaction model.

On the contrary, the morphology of  $Na_2SiO_3$  prepared by precipitation was totally different. In this case,  $Na_2SiO_3$  seemed to

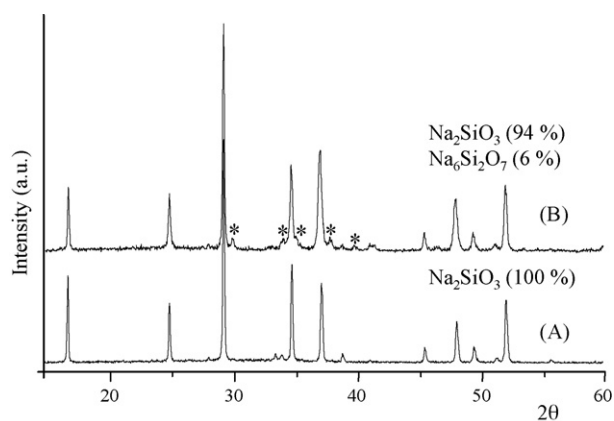


**Fig. 1.** XRD patterns of the  $Na_2SiO_3$  samples prepared by solid-state reaction (A) and precipitation (B). Peaks labeled as (\*) correspond to the  $Na_6Si_2O_7$  phase and the percentage of each phase is indicated into parenthesis.

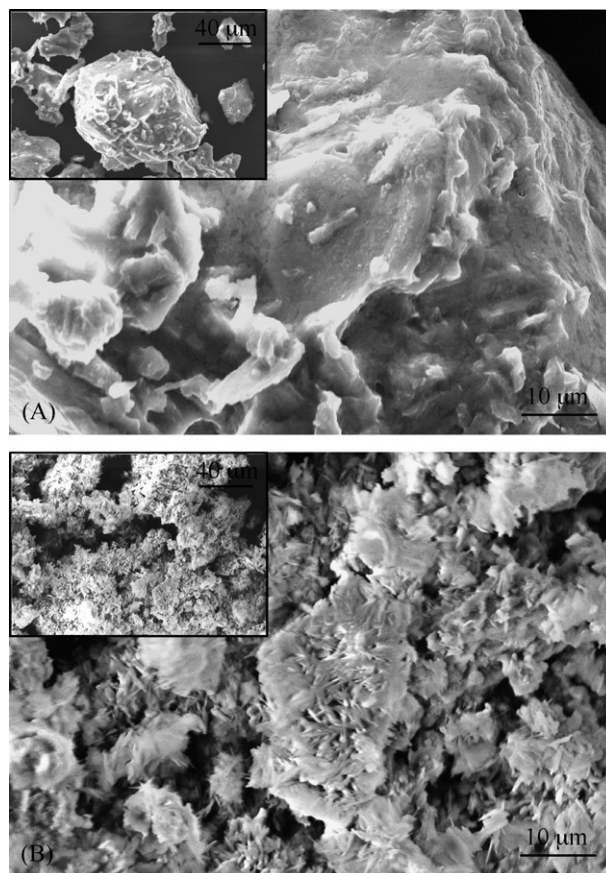


**Fig. 2.** SEM images of  $Na_2SiO_3$  samples prepared by solid-state reaction at  $900^\circ C$  for 4 h (A) and prepared by precipitation without any thermal treatment (B).

agglomerate in particles of  $5\text{--}20\ \mu m$ , where the agglomerates were formed by some kind of laminar or filament particles (Fig. 2B). Therefore, the agglomerates are highly porous. It seems that the precipitation process is promoting the union of several  $Na_2SiO_3$  chains, resulting in the formation of this kind of structures.  $Na_2SiO_3$  is a chain of many  $(SiO_3)^{2-}$  molecules, produced by the conjugation of a large number of  $(SiO_4)^{4-}$  tetrahedrons linked by two oxygen atoms among them [15]. Thus, several of this  $Na_2SiO_3$  chains must be linked, producing filament-like structures. The SEM results were supported by a surface area analyses. While the solid-state sample had a surface area of  $1.35\ m^2/g$ , the precipitation sample had a larger area,  $6.25\ m^2/g$ . Although none of the samples presented significant surface areas, the samples prepared by precipitation have up to four times more area than the sample prepared by solid state.

Once, the samples were characterized, the thermal behavior of  $Na_2SiO_3$ , into a flux of  $CO_2$ , was studied. Initially, the sample prepared by solid-state reaction was chosen in order to have similar geometry and particle size than those characteristics presented by other materials in similar studies [6–11]. Thermogravimetric analysis of  $Na_2SiO_3$  into a flux of carbon dioxide ( $CO_2$ ) is shown in Fig. 3. The thermogram only showed a small weight increment between room temperature and  $130^\circ C$ , which was attributed to a  $CO_2$  sorption process. After that, the sample started losing weight in two different processes, one between  $130^\circ C$  and  $700^\circ C$ , and another one between  $700^\circ C$  and  $920^\circ C$ . The total weight lost was equal to 9 wt%. These processes were associated to dehydroxylation and decarbonation of the sample, as usually sodium ceramic are highly hydroscopic. The  $CO_2$  chemisorption at low temperatures was confirmed by XRD, as follows:  $Na_2SiO_3$  powder was heat treated up to  $130^\circ C$  into a flux of  $CO_2$ , and then, the heating process was

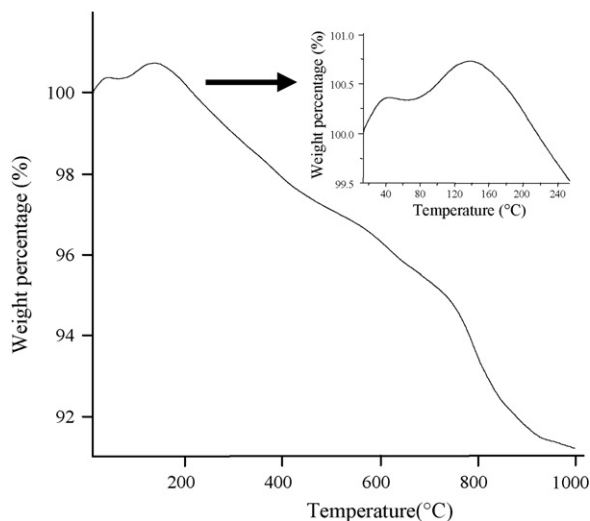


Fig. 3. Thermogravimetric analysis of the  $\text{Na}_2\text{SiO}_3$  into a flux of  $\text{CO}_2$ .

stopped. The XRD pattern showed the formation of small quantities of  $\text{Na}_2\text{CO}_3$ , 5% (data not shown).

$\text{Na}_2\text{SiO}_3$ , under a flux of  $\text{CO}_2$ , presented a totally different behavior than that observed on other alkaline ceramics such as  $\text{Li}_4\text{SiO}_4$ ,  $\text{Li}_2\text{ZrO}_3$ ,  $\text{Na}_2\text{ZrO}_3$  and  $\text{Li}_2\text{O}$  [1,2,7,11–13]. All these materials absorb  $\text{CO}_2$  at different ranges of temperatures, and they can retain high quantities of  $\text{CO}_2$ . On the contrary,  $\text{Na}_2\text{SiO}_3$  only absorbed  $\approx 1$ –2 wt%, and the absorption was produced at low temperatures. Nevertheless, this result is coherent with the results reported for  $\text{Li}_2\text{SiO}_3$ , which apparently is not able to absorb  $\text{CO}_2$  either [14]. In this case,  $\text{Na}_2\text{SiO}_3$  absorbed small quantities of  $\text{CO}_2$ , in the agreement with the reports that indicates that in general sodium ceramics are more reactive than lithium ceramics [9].

In order to obtain some kinetic information about the  $\text{CO}_2$  sorption, additional isothermal analyses were performed. Fig. 4 shows the isothermal graphs of  $\text{Na}_2\text{SiO}_3$  heat-treated at different temperatures into a flux of  $\text{CO}_2$ . The sorption rates presented similar behaviors at the three different temperatures, and data fitted to a double exponential model:  $y = A \exp(-k_1 t) + B \exp(-k_2 t) + C$ , where,  $y$  represents the percentage of weight increased due to  $\text{CO}_2$  absorption,  $t$  is the time,  $k_1$  and  $k_2$  are the rate constants and  $A$ ,  $B$

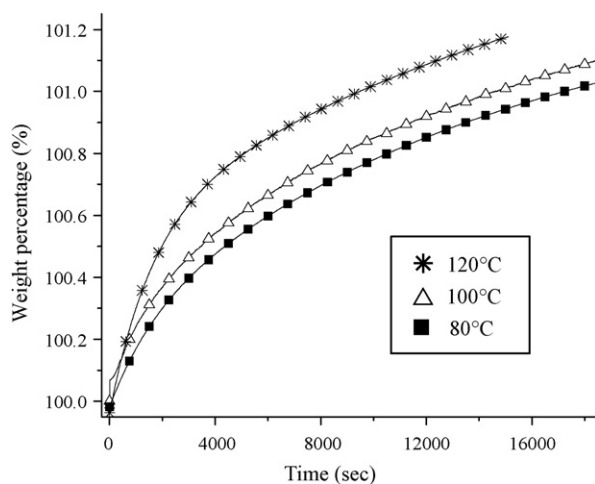


Fig. 4. Isotherms of  $\text{CO}_2$  sorption on  $\text{Na}_2\text{SiO}_3$  heat-treated at  $80^\circ\text{C}$ ,  $100^\circ\text{C}$  and  $120^\circ\text{C}$  into a flux of  $\text{CO}_2$ . The symbols correspond to the experimental data, and the lines correspond to the double exponential fit.

Table 1

Kinetic parameters obtained from the experimental data fitted to a double exponential model

Parameter	Temperature ( $^\circ\text{C}$ )		
	80	100	120
$k_1$ (1/s)	1.2786	2.0589	2.3304
$k_2$ (1/s)	0.0894	0.2108	0.2022
$A$	-1.1194	-1.5088	-1.1031
$B$	-0.2506	-0.2361	-0.5841
$C$	101.3	101.7	101.6
$R^2$	0.99972	0.99997	0.99933

and  $C$  are the pre-exponential factors. This model has been used in other alkaline ceramics to describe the  $\text{CO}_2$  chemisorption and alkaline diffusion process simultaneously, obtaining two different rate constants values;  $k_1$  for the chemisorption process and  $k_2$  for the diffusion process [7,9]. The values obtained at each temperature are presented in Table 1. As the data adjusted to a double exponential model, it means that there are two different processes associated, as in some other alkaline ceramics, a chemisorption and diffusion processes [7,9]. Then,  $\text{Na}_2\text{SiO}_3$  reacts with  $\text{CO}_2$ , producing an external layer of  $\text{Na}_2\text{CO}_3$ , and after that, sodium must have to diffuse throughout the carbonate layer to be able to react with the  $\text{CO}_2$ . In this case,  $k_1$  (chemisorption process) is one order of magnitude larger than  $k_2$  (diffusion process). Therefore, kinetically the limiting step of the whole process is the diffusion. Then, the poor  $\text{CO}_2$  sorption results may be attributed the structural or packing factors of the  $\text{Na}_2\text{SiO}_3$  crystal structure, which should inhibit sodium diffusion. For a model of these characteristics, if the kinetic constant values ( $k_1$  and  $k_2$ ) are linear dependent with temperature, the gradients of these best-fit lines should follow an Arrhenius-type behavior. Fig. 5 shows the plots of  $\ln k$  versus  $1/T$ , where linear trends are observed for both processes. The fitting observed for both graphs varied significantly. While the chemisorption process fitted excellent ( $\ln k_1$  vs.  $1/T$ ), it was not the case on the diffusion process ( $\ln k_2$  vs.  $1/T$ ). It may be explained due to interference produced by the chemisorption process, which occurs firstly. Another explanation would be that the diffusion process does not follow the Arrhenius-type behavior. Anyway, the activation energies for the  $\text{CO}_2$  absorption (chemisorption) on  $\text{Na}_2\text{SiO}_3$  and sodium diffusion were estimated to be 17,482 J/mol and 23,968 J/mol, respectively.

The  $\text{CO}_2$  capture capacity of this sample was extremely poor, in comparison with other ceramics. For example,  $\text{Na}_2\text{ZrO}_3$ , which is

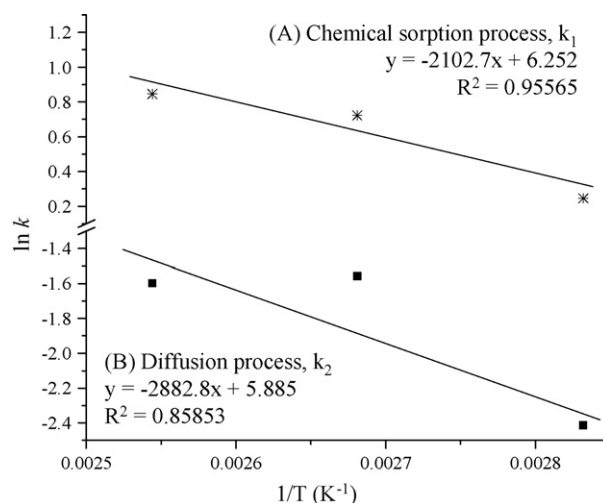
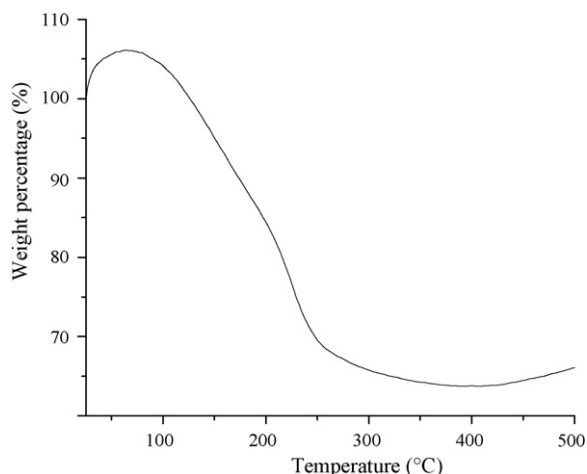


Fig. 5. Plots of  $\ln k$  vs.  $1/T$ , for the two different processes observed on the  $\text{CO}_2$  sorption on  $\text{Na}_2\text{SiO}_3$ .



**Fig. 6.** Thermogravimetric analysis of the  $\text{Na}_2\text{SiO}_3$  prepared by the precipitation method, into a flux of  $\text{CO}_2$ .

an isostructural ceramic, do absorb  $\text{CO}_2$  [9,16]. In this case,  $\text{Na}_2\text{ZrO}_3$  begins the  $\text{CO}_2$  absorption at low temperatures as well. Nevertheless, in this case, the absorption continues through the bulk of the ceramic. In other words, the  $\text{CO}_2$  absorption is not limited to the surface or by sodium diffusion. On the other hand, it has been proved, for other materials, that the particle size and surface area play very important roles on the  $\text{CO}_2$  capture [7,17]. Therefore, it could be interesting to analyze this material with different particle size and surface area. Therefore, although the  $\text{Na}_2\text{SiO}_3$  sample prepared by the precipitation method was not pure (see XRD results), it was used to analyze its  $\text{CO}_2$  capture capacity, because it has a smaller particle size and the larger surface area. The thermogram of this sample, into a flux of  $\text{CO}_2$ , showed a similar behavior than that observed for the sample with solid-state reaction (Fig. 6). The thermogram presented a similar trend, where the only significant difference was the quantity of  $\text{CO}_2$  trapped. In this case, the amount of  $\text{CO}_2$  absorbed was 6 wt%. It means three times more  $\text{CO}_2$  than that absorbed on the solid-state sample. The increment observed on this analysis could be explained as a function of the particle size and surface area of the samples. As the sample prepared by precipitation has a larger surface area, there must be more sodium atoms at the surface of the particles, enabling the  $\text{Na}_2\text{CO}_3$  formation. Furthermore, as particles are smaller and there is the presence of porosity, these factors may increase the vapor pressures into the porous, grain boundaries and triple points produced by the junction of several particles, increasing the reactivity. Conversely, the thermal stability of this sample was highly modified. After the  $\text{CO}_2$  sorption 30 wt% was lost, which may be partially attributed to decarbonation and sodium sublimation processes. In this case, perhaps as there is more sodium atoms present at the surface, it may be presented some sodium sublima-

tion at high temperatures, which contributed to the loss of weight as well.

#### 4. Conclusion

The  $\text{CO}_2$  chemisorption kinetics, of  $\text{Na}_2\text{SiO}_3$ , was analyzed in this work. Later the particle size effect was investigated as well.  $\text{CO}_2$  sorption analyses showed that  $\text{Na}_2\text{SiO}_3$  has the capacity to absorb  $\text{CO}_2$  between room temperature and  $130^\circ\text{C}$ . The quantity of  $\text{CO}_2$  absorbed is not high enough to utilize this ceramic as  $\text{CO}_2$  captor. Nevertheless, it was performed the kinetic analysis of the  $\text{CO}_2$  sorption. The results indicate that sorption mechanism occurs through a double-step process; superficial chemical sorption and sodium diffusion processes, where the diffusion process is the limiting step. The activation energies for the  $\text{CO}_2$  chemical sorption and the diffusion of sodium were estimated to be  $17,482\text{ J/mol}$  and  $23,968\text{ J/mol}$ , respectively. Finally, it was observed that particle size and surface area play very important roles during the  $\text{CO}_2$  capture.

It has to be pointed out that, although the  $\text{CO}_2$  absorption observed in  $\text{Na}_2\text{SiO}_3$  is considerably small, this material absorbed more  $\text{CO}_2$  than its lithium isostructural ceramic,  $\text{Li}_2\text{SiO}_3$ . Again, sodium ceramics show to be better  $\text{CO}_2$  absorbents, in comparison to lithium ceramics, as the zirconates case ( $\text{Li}_2\text{ZrO}_3$  and  $\text{Na}_2\text{ZrO}_3$ ).

#### Acknowledgements

This work was financially supported by the project PAPIIT-UNAM IN103506. Furthermore, authors thank to L. Baños, J. Guzman and E. Fregoso for technical help in the XRD, SEM and thermal analyses, respectively.

#### References

- [1] K. Essaki, K. Nakagawa, M. Kato, H. Uemoto, *J. Chem. Eng. Jpn.* 37 (2004) 772–777.
- [2] C. Gauer, W. Heschel, *J. Mater. Sci.* 41 (2006) 2405–2409.
- [3] K. Nakagawa, T. Ohashi, *J. Electrochem. Soc.* 145 (1998) 1344–1346.
- [4] R. Xiong, J. Ida, Y.S. Lin, *Chem. Eng. Sci.* 58 (2003) 4377–4385.
- [5] J.I. Ida, R. Xiong, Y.S. Lin, *Sep. Purif. Technol.* 36 (2004) 41–51.
- [6] M. Kato, K. Nakagawa, K. Essaki, Y. Maezawa, Sh. Takeda, R. Kogo, Y. Hagiwara, *Int. J. Appl. Ceram. Technol.* 2 (2005) 467–475.
- [7] M. Venegas, E. Fregoso-Israel, H. Pfeiffer, *Ind. Eng. Chem. Res.* 46 (2007) 2407–2412.
- [8] H.A. Mosqueda, C. Vazquez, P. Bosch, H. Pfeiffer, *Chem. Mater.* 18 (2006) 2307–2310.
- [9] H. Pfeiffer, C. Vazquez, V.H. Lara, P. Bosch, *Chem. Mater.* 19 (2007) 922–926.
- [10] H. Pfeiffer, P. Bosch, *Chem. Mater.* 17 (2005) 1704–1710.
- [11] M. Kato, S. Yoshikawa, K. Nakagawa, *J. Mater. Sci. Lett.* 21 (2002) 485–487.
- [12] K. Essaki, M. Kato, H. Uemoto, *J. Mater. Sci.* 21 (2005) 5017–5019.
- [13] M. Escobedo-Bretado, V. Guzmán-Velderrain, D. Lardizábal-Gutiérrez, V. Collins-Martínez, A. Lopez-Ortiz, *Catal. Today* 107–108 (2005) 863–867.
- [14] M. Kato, K. Nakagawa, *J. Ceram. Soc. Jpn.* 109 (2001) 911–914.
- [15] C.J. Brinker, G.W. Scherer, *Sol–Gel Science, the Physics and Chemistry of the Sol–Gel Processing*, Academic Press, Inc., United States of America, 1990.
- [16] I. Alcérreca-Corte, E. Fregoso-Israel, H. Pfeiffer, *J. Phys. Chem. C* 112 (2008) 6520–6525.
- [17] K.H. Choi, Y. Korai, I. Mochida, *Chem. Lett.* 32 (2003) 924–925.